



Remarkably high blue ring occurrence in Estonian Scots pines in 1976 reveals wood anatomical evidence of extreme autumnal cooling

Ciara Greaves¹ · Alan Crivellaro^{1,2} · Alma Piermattei¹ · Paul J. Krusic^{1,3} · Clive Oppenheimer¹ · Aleksei Potapov⁴ · Maris Hordo⁴ · Sandra Metslaid⁴ · Regino Kask⁴ · Ahto Kangur⁴ · Ulf Büntgen^{1,5,6,7}

Received: 5 July 2022 / Accepted: 3 November 2022 / Published online: 21 November 2022
© The Author(s) 2022

Abstract

Key message An exceptionally high number of blue rings were formed within and between Scots pine trees from Estonia in 1976: a year that is well known for its outstanding summer heatwave over Western Europe, but its extreme autumnal cooling over Eastern Europe has so far been neglected in scientific literature.

Abstract ‘Blue rings’ (BRs) are visual indicators of less lignified cell walls typically formed towards the end of a tree’s growing season. Though BRs have been associated with ephemeral surface cooling, often following large volcanic eruptions, the intensity of cold spells necessary to produce BRs, as well as the consistency of their formation within and between trees still remains uncertain. Here, we report an exceptionally high BR occurrence within and between Scots pine (*Pinus sylvestris* L.) trees at two sites in Estonia, including the first published whole-stem analysis for BRs. Daily meteorological measurements from a nearby station allowed us to investigate the role temperature has played in BR formation since the beginning of the twentieth century. The single year in which BRs were consistently formed within and amongst most trees was 1976. While the summer of 1976 is well known for an exceptional heatwave in Northwest Europe, mean September and October temperatures were remarkably low over Eastern Europe, and 3.8 °C below the 1961–1990 mean at our sites. Our findings contribute to a better eco-physiological interpretation of BRs, and further demonstrate their ability to reveal ephemeral cooling not captured by dendrochronological ring width and latewood density measurements.

Keywords Climate change · Dendrochronology · Europe · Lignification · *Pinus sylvestris* · Temperature reconstruction · Wood anatomy

Communicated by E. van der Maaten.

✉ Ciara Greaves
ccg39@cam.ac.uk

¹ Department of Geography, University of Cambridge, Cambridge CB2 3EN, UK

² Forest Biometrics Laboratory, Faculty of Forestry, “Stefan Cel Mare” University of Suceava, 720229 Suceava, Romania

³ Department of Physical Geography, Stockholm University, 10691 Stockholm, Sweden

⁴ Chair of Forest and Land Management and Wood Processing Technologies, Institute of Forestry and Engineering, Estonian University of Life Sciences, 51006 Tartu, Estonia

⁵ Global Change Research Institute of the Czech Academy of Sciences (CzechGlobe), 603 00 Brno, Czech Republic

⁶ Department of Geography, Faculty of Science, Masaryk University, 613 00 Brno, Czech Republic

⁷ Swiss Federal Research Institute WSL, 8903 Birmensdorf, Switzerland

Introduction

BRs are wood anatomical anomalies identified in conifers that reflect abrupt cold spells during the growing season (Piermattei et al. 2015, 2020). By double-staining wood thin sections with an aqueous solution of Safranin and Astra Blue (Gerlach 1984; Schweingruber 2007), cell walls lacking lignin stain blue whilst lignified cell walls stain red. Latewood axial tracheids which would normally be fully lignified (red stained), are completely or partially non-lignified in BRs (blue-stained). Cell wall lignification has been found to be inhibited by low temperatures, most notably towards the end of the growing season (Gindl et al. 2000; Crivellaro and Büntgen 2020; Crivellaro et al. 2022). These cold spells could be as short as a couple of weeks or even a few days and are not detectable with quantitative wood anatomy measurements (Piermattei et al. 2020; Björklund et al. 2021), or dendrochronological parameters such as tree-ring width (TRW)

(Fritts 1976), maximum latewood density (MXD) (Parker and Jozca 1973; Schweingruber et al. 1978), or MXD's surrogate blue intensity (BI) (McCarroll et al. 2002; Björklund et al. 2019).

Up to now, BRs along with their years of occurrence have been found in *Pinus nigra* in the Apennines, Italy (Piermattei et al. 2015; Crivellaro et al. 2018), *Pinus sylvestris* in Romania (Semeniuc et al. 2016), Latvia (Matisons et al. 2020), Finland (Björklund et al. 2021) and Poland (Matulewski et al. 2022), *Pinus contorta* in Western Canada and the US (Montwé et al. 2018), *Pinus uncinata* in the Spanish Pyrenees (Piermattei et al. 2020), *Pinus longaeva* in Nevada, US (Tardif et al. 2020), and *Larix decidua* in the Russian Altai (Büntgen et al. 2020).

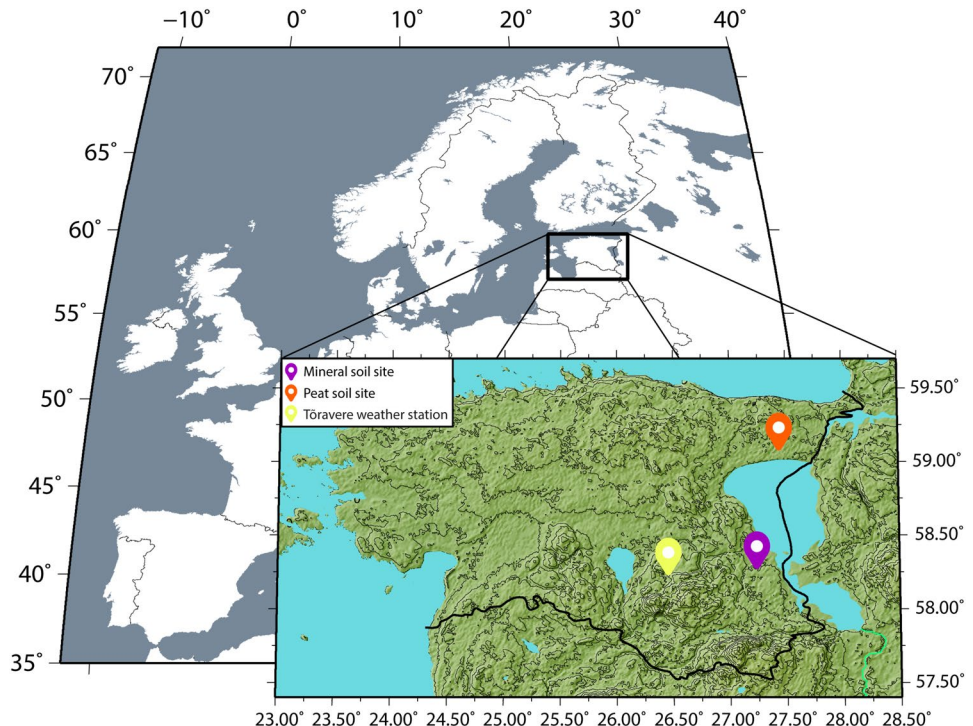
Although BRs indicate potential for capturing ephemeral cooling events towards the end of the growing season (e.g., related to volcanic forcing of climate; Piermattei et al. 2020; Büntgen et al. 2020; Tardif et al. 2020), little is known of the intensity of cooling needed to generate a BR. Such insights will advance the potential use of BRs as a high-resolution climate proxy (Piermattei et al. 2020). Furthermore, it is not known how consistent BR formation is within trees, both around the circumference of a tree stem and along its height. Our aim here is to address these points through BR identification in samples from 14 living Scots pines in Estonia, for which local daily temperature measurements are available spanning the interval of 1901–2019. We describe the distribution and abundance of BRs within and between trees, in relation to TRW and BI measurements from the same trees.

Materials and methods

The study area comprises of two sites in Estonia where hemiboreal forests prevail (Fig. 1). A total of 14 Scots pine trees were sampled during previous studies (Metslaid et al. 2011; Potapov et al. 2019). Ten trees were growing on mesic mineral soil in Järvselja (58.318° N, 27.273° E; 33–35 m a.s.l) with an average height and age of 29.3 m and 63 years respectively, and four trees on peat soil in Ongassaare (59.148° N, 27.428° E; 44–50 m a.s.l) with an average height and age of 22.6 m and 119 years (Fig. 2). At the mineral soil site, the ten trees were felled and whole-stem disks were taken at 1.3 m above ground. From each of these ten disks, a single radial rectangular slat ~ 1.5 cm wide, and as thick as the disk, extending from the pith to bark was removed. Five of the ten mineral site trees, ranging from 20 to 35 m in height, were additionally cut every 2.5 m from ground level. From these five trees' whole-stem disks, eight radial slats were cut every 45° beginning in the direction of North (0°), and progressing clockwise around the stem to the Northeast (45°), East (90°), Southeast (135°), etc. (Fig. 2). At the peat soil site, four trees were sampled at 1.3 m using a 5.4 mm-diameter increment borer.

Prior to the anatomical analysis all radial samples were prepared for micrometer measurement at a resolution of 0.01 mm (Krusic et al. 1987), and the resulting time-series of radial TRW were cross-dated using the program

Fig. 1 Map of Europe with black box covering Estonia and surrounding area. Topographic map of Estonia, with mineral and peat soil study sites (purple and orange markers respectively), and Tõravere meteorological station (yellow marker)



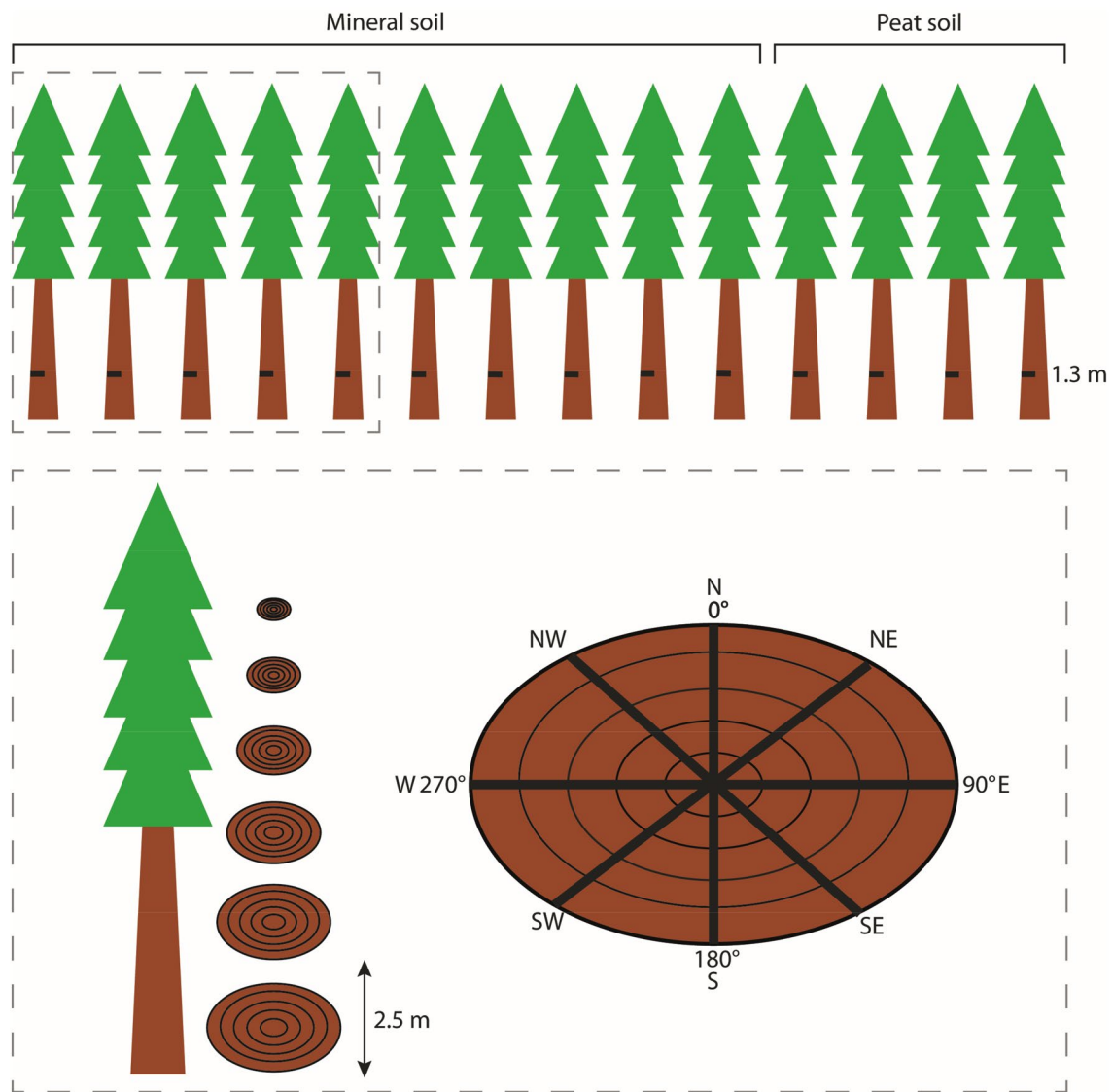


Fig. 2 The 14 Scots pine trees each sampled at 1.3 m are shown at the top; ten from mineral soil sites and four from peat soil sites. The five trees in the grey dashed square are the trees where further sampling occurred, this is illustrated in the box below; disks are shown to

be taken from each tree from ground level to the apex at every 2.5 m stem height, each disk is then shown to be sampled at eight radii (N, NE, E, SE, S, SW, W and NW)

COFECHA (Holmes 1983). From three of the whole-stem sectioned trees at the mineral soil site only, annually resolved BI measurements were obtained from all southern (180°) radii, at every height along the stems. Samples were treated with ethanol (98%) for eight hours in a Soxhlet to remove resins, then sanded and scanned using an Epson V850 Pro Scanner. The program CooRecorder was used to generate BI measurements (Rhdval et al. 2014; Maxwell and Larsson 2021). Both the TRW and BI measurements

were detrended using a negative exponential curve, and ARSTAN chronologies (Cook 1985) were produced using the program ARSTAN (Cook et al. 2017).

A core microtome was used to cut 20–30 μm -thick sections from each radial sample (Gärtner and Nievergelt 2010; Gärtner et al. 2015). Each thin section was then double-stained with a mixture of Safranin and Astra Blue to expose lignified (red) and less-lignified (blue) cell walls (Gerlach 1984; Schweingruber 2007). To prepare the staining

solutions, 0.1 g of Safranin was dissolved in 100 ml of distilled water, and 0.5 g of Astra Blue was dissolved in 100 ml of distilled water along with 2.0 ml of acetic acid. The Astra Blue and Safranin solutions were then combined at a ratio of 4:1 (four parts Astra Blue to one part Safranin). Once cut and stained, the thin sections were washed with distilled water to remove excess stain, placed on a glass slide, and secured with a cover slip. A compound microscope was used to find BRs in each section, which were defined as any ring containing blue (less-lignified) or partly blue cell walls (Fig. 3).

Daily temperature measurements since 1901 from the Tõravere meteorological station, which is located 47 km from the mineral site and 92 km from the peat site, were

extracted from KNMI Climate Explorer (<http://climexp.knmi.nl/>). The Tõravere station was chosen for its proximity to the sites and long temperature records. Since this study is investigating the impact of extreme weather events on plants at the cellular level, minimum daily temperatures were used (Schenker et al. 2014; Körner 2021). As previous studies have suggested reduced cell wall lignification is associated with low late growing season temperatures (Piermattei et al. 2015, 2020; Semeniuc et al. 2016; Montwé et al. 2018; Matisons et al. 2020; Tardif et al. 2020; Matulewski et al. 2022), the thermal conditions at the end of the growing season were the main focus of this study. The September–October interval was selected for temperature analysis since this time period has been associated with cell wall lignification of

Fig. 3 BRs with varying cell wall lignification levels imaged at $\times 40$ magnification with zoom, from transverse double-stained thin sections of Scots pine. Lignified cells are stained red and non-lignified cells are blue, the extent of blue cell walls increases from (a) to (c), indicating decreasing cell wall lignification

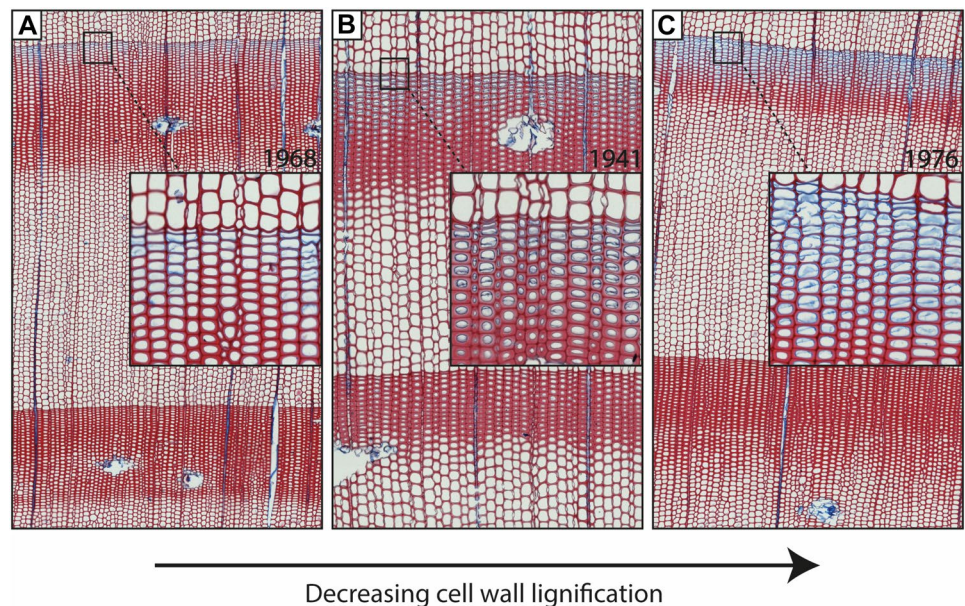
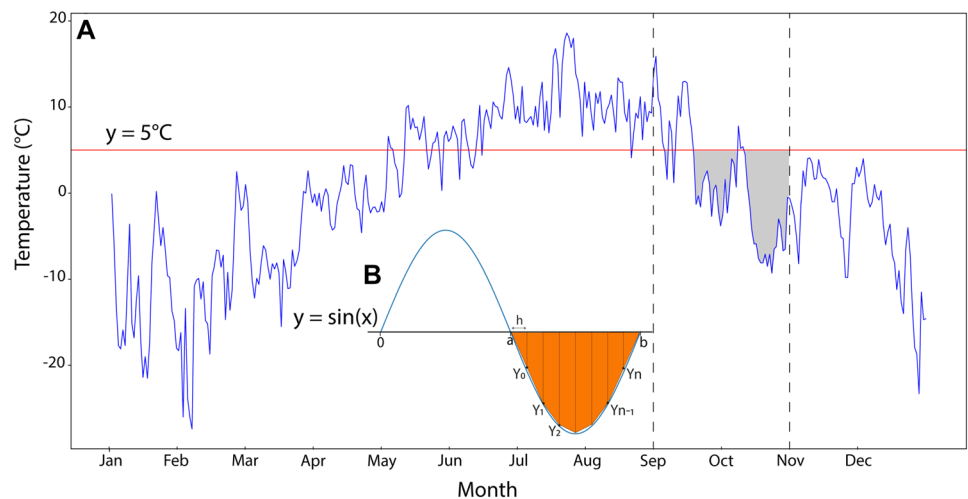


Fig. 4 **a** Daily minimum temperatures from 1976 (Tõravere meteorological station) with 5°C temperature threshold line (red). The boundaries of the below threshold cold period of interest (September–October) are labelled with dashed lines. The below 5°C grey shaded area represents the region where the area will be approximated by trapezoidal integration. **b** Example of trapezoidal integration on a sine wave, trapezoids are drawn between a and b the curve, their heights (Y_0, Y_1, \dots, Y_n), and widths (h) are labelled



latewood tracheids in conifers in Northern Hemisphere mid-latitudes (Gindl et al. 2000; Rossi et al. 2006).

Two methods were used to describe the degree of variability in late growing-season temperatures at our sites. First, average minimum daily temperatures for the period September to October (61 days) were calculated for each year from 1901 to 2019. The second method utilised the trapezoidal rule (Yeh and Kwan 1978). Here the trapezoidal rule is used to estimate the degree of plant exposure to September–October daily minimum temperatures, below a specified threshold, between 1901 and 2019 (Fig. 4). In this study, 5 °C was used as an approximated threshold for cambial division in tree line species (Cabon et al. 2020; Tumajer et al. 2021; Körner 2008, 2021). The trapezoidal integration method effectively excludes all warm weather signals, focusing only on cold periods (below 5 °C threshold) at daily resolution. Since cold temperatures are of interest to this study, given their link to lignification and BR formation (Piermattei et al. 2015), this method is suitable for producing results which are not diluted by warm temperature signals, unlike the monthly averages which

encompass cold and warm periods. The following equation was used to compute areas between minimum temperature curves and the 5 °C threshold:

$$\int_a^b y dx \approx \frac{1}{2} h \{ (y_0 + y_n) + 2(y_1 + y_2 + \dots + y_{n-1}) \}, \quad (1)$$

where

$$h = \frac{b - a}{n}. \quad (2)$$

The variables, a and b are the start and end of the time period of interest (1st of September and 31st of October), n is the number of trapezoids and $y_0, y_1 \dots y_n$ are the absolute heights of each trapezoid (Fig. 4b).

For analysis of temperature anomalies on the continental scale, we used Version 4.05 of the gridded (0.5° by 0.5°) CRU TS dataset (Harris et al. 2020), focussing on the June–August (JJA) and September–October (SO) temperature anomalies, with respect to the 1961–90 mean, calculated for the 4878 grid cells over Europe.

Fig. 5 **a** Number of BRs recorded in 1.3 m samples from 14 trees over the period of 1854–2019. Sample depth is indicated by frequency of trees (black line). **b** Number of BRs recorded from measurement radii taken along the tree stem from five trees over the period of 1894–2008. Sample depth is indicated by number of measurement radii (black line)

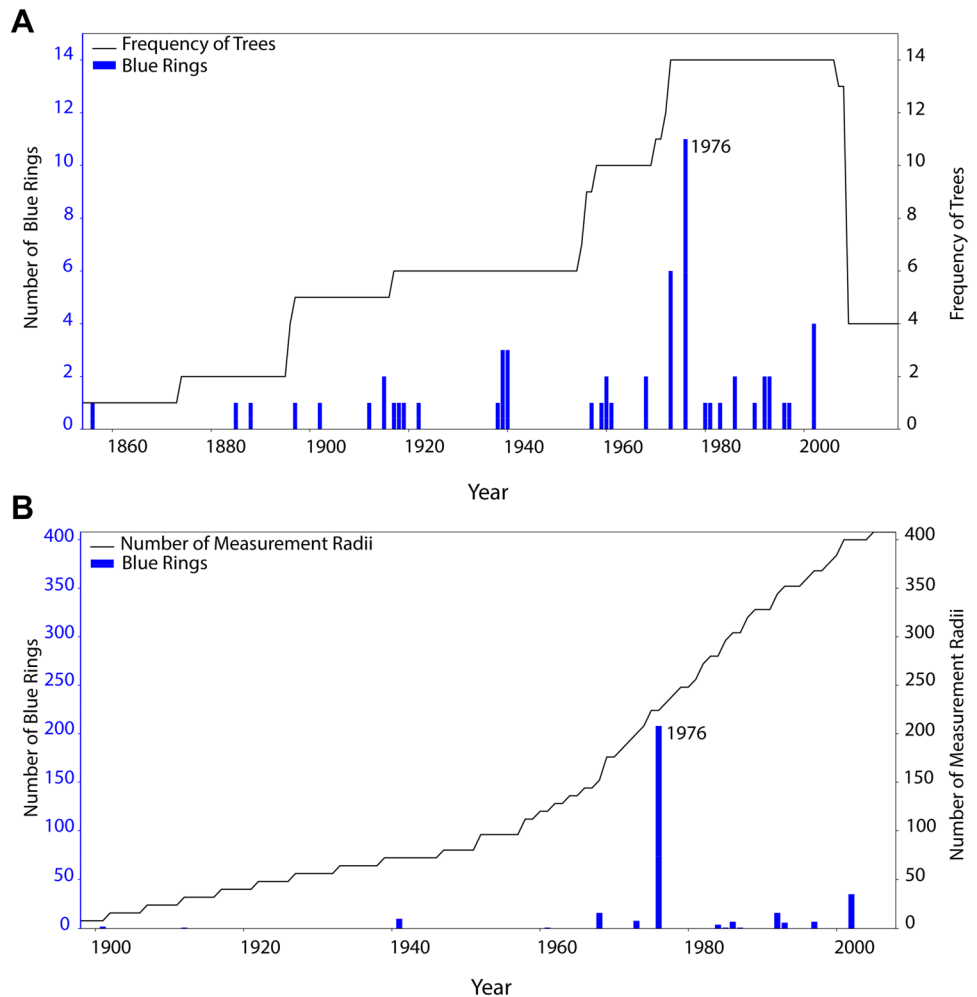


Table 1 Blue Rings (BRs) recorded in 1.3 m samples from 14 trees over the period of 1854–2019: calendar year, sample depth, number of BRs (no. BRs) and percentage of BRs (% BRs) are indicated. The dataset is sorted in descending order according to no. BRs

Year	Sample depth	No. BRs	% BRs
1976	14	11	78.6
1973	14	6	42.9
2002	14	4	28.6
1939	6	3	50.0
1940	6	3	50.0
1915	5	2	40.0
1960	10	2	20.0
1968	10	2	20.0
1986	14	2	14.3
1992	14	2	14.3
1993	14	2	14.3
1856	1	1	100.0
1885	2	1	50.0
1888	2	1	50.0
1897	5	1	20.0
1902	5	1	20.0
1912	5	1	20.0
1917	6	1	16.7
1918	6	1	16.7
1919	6	1	16.7
1922	6	1	16.7
1938	6	1	16.7
1957	9	1	11.1
1959	10	1	10.0
1961	10	1	10.0
1980	14	1	7.1
1981	14	1	7.1
1983	14	1	7.1
1990	14	1	7.1
1996	14	1	7.1
1997	14	1	7.1

The North Atlantic Oscillation (NAO) was also investigated to identify BR years with anomalous atmospheric conditions. A dataset of monthly NAO index values, derived from the normalised pressure differences between Iceland (Reykjavik) and the Azores (Ponta Delgada) from 1901 to 2019, was obtained from the University of East Anglia Climate Research Unit (Jones et al. 1997; <https://crudata.uea.ac.uk/cru/data/nao/>). The NAO median, interquartile ranges, and outliers for each month between 1901 and 2019 were calculated from this dataset.

Finally, the TRW and BI ARSTAN chronologies were correlated with monthly mean temperatures. The purpose of this test was to determine whether the TRW and BI indexes from our sites contain any growing-season temperature signals. This analysis was undertaken using the

Table 2 Blue Rings (BRs) recorded in samples from measurement radii taken along the tree stem from five trees over the period of 1898–2008: calendar year, sample depth, number of BRs (no. BRs) and percentage of BRs (% BRs) are indicated. The dataset is sorted in descending order according to no. BRs

Year	Sample depth	No. BRs	% BRs
1976	224	208	92.9
2002	400	35	8.8
1968	152	16	10.5
1992	344	16	4.7
1941	72	10	13.9
1973	200	8	4.0
1986	304	7	2.3
1997	368	7	1.9
1993	352	6	1.7
1984	280	4	1.4
1901	8	2	25.0
1912	32	1	3.1
1961	120	1	0.8
1985	296	1	0.3
1987	304	1	0.3

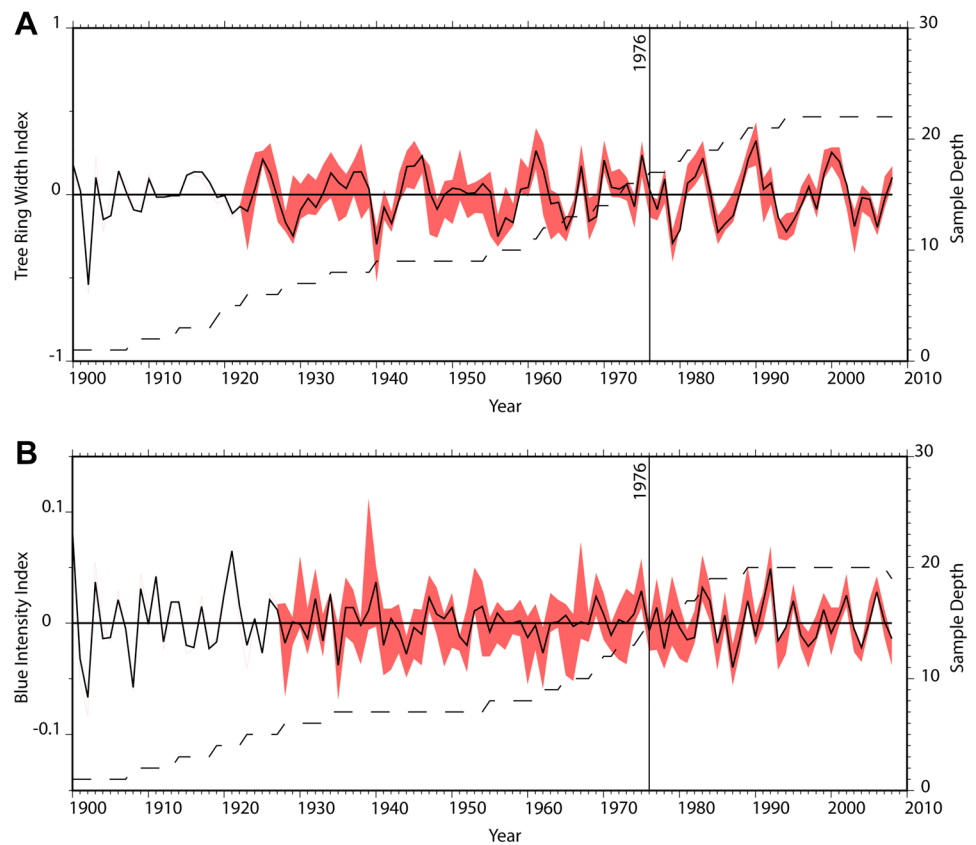
KNMI Climate Explorer (<http://climexp.knmi.nl/>). Daily temperature values from the Tõravere meteorological station (1901–2019) were averaged into mean monthly temperatures, which were used to calculate Pearson's correlation coefficients with the TRW and BI indexes. Both original and pre-whitened ARSTAN correlations were produced.

Results

Out of 1121 annual rings from 1.3 m stem height that span the period 1854–2019 (Fig. 5a; Table 1), 59 were classified as BRs (5.3%). Thirty-one calendar years were identified in which a BR was found in at least one tree. In 1938 and 1940 50% of the trees sampled produced a BR, 42.9% in 1973, and 28.6% in 2002. The most remarkable year is 1976 with 78.6% of trees yielding BRs.

From the five whole-stem trees sampled 16,872 annual rings were analysed from 1898 to 2008 (Fig. 2), and a total of 323 BRs (1.9%) identified. The 1976 BR was the only BR found at nearly every sampling height and direction (Fig. 5b), present in 92.9% of the studied radii. BRs were present in all the 1976 rings in four of the five trees sampled, the exception being one tree where the 1976 BRs were absent in two of 12 disks, at 7.5 and 32.5 m from ground level. Apart from 1976, 14 other distinct BRs were identified (Fig. 5b; Table 2). However, these additional BRs were sparse with respect to the sample depth and were distributed unevenly, both in height along the stem and orientation.

Fig. 6 ARSTAN Chronologies of tree-ring width (a) and blue intensity (b) from 1898 to 2008, sample depth is indicated by the dashed line and the year 1976 is marked with a vertical line labelled. The red shaded area indicates 95% bootstrap confidence interval



The TRW and BI ARSTAN chronologies are shown in Fig. 6. The TRW index value for 1976 is -0.036 , with a z score of -0.25 . Similarly, for BI, the index value of 1976 is -0.005 , with a z score of -0.26 .

The average September and October minimum temperatures from 1901 to 2019 ranged from 1.2 to 8.2 °C, with a mean and SD of 5.0 and 1.4 °C, respectively (Fig. 7a). The average minimum September and October temperature for all the years for which we recorded BRs is 4.4 °C (z score = -0.39). The lowest temperature value in the dataset is from 1976 (1.2 °C), this value has a z score of -2.65 .

The trapezoidal integration values for September and October from 1901 to 2019 range from 26.3 to 156.6 , the mean value is 70.1 , with a SD of 22.7 (Fig. 7b). The average trapezoidal integration value for all the years where BRs are recorded is 82.0 (z score = 0.43). The value for 1976 is the largest (156.6), representing the most substantial cooling, <5 °C, from September to October. The 1976 result has a z score of 3.80 , representing a significant outlier, whilst this is not the case for the average September–October temperature in 1976.

Although the summer of 1976 saw a heatwave in north-west Europe, summer temperatures at our study sites in Estonia were below average (Fig. 8a). However, September and October (late growing season) temperatures were somewhat

cooler than average over much of Europe, and particularly low for our sites in Estonia (Fig. 8b).

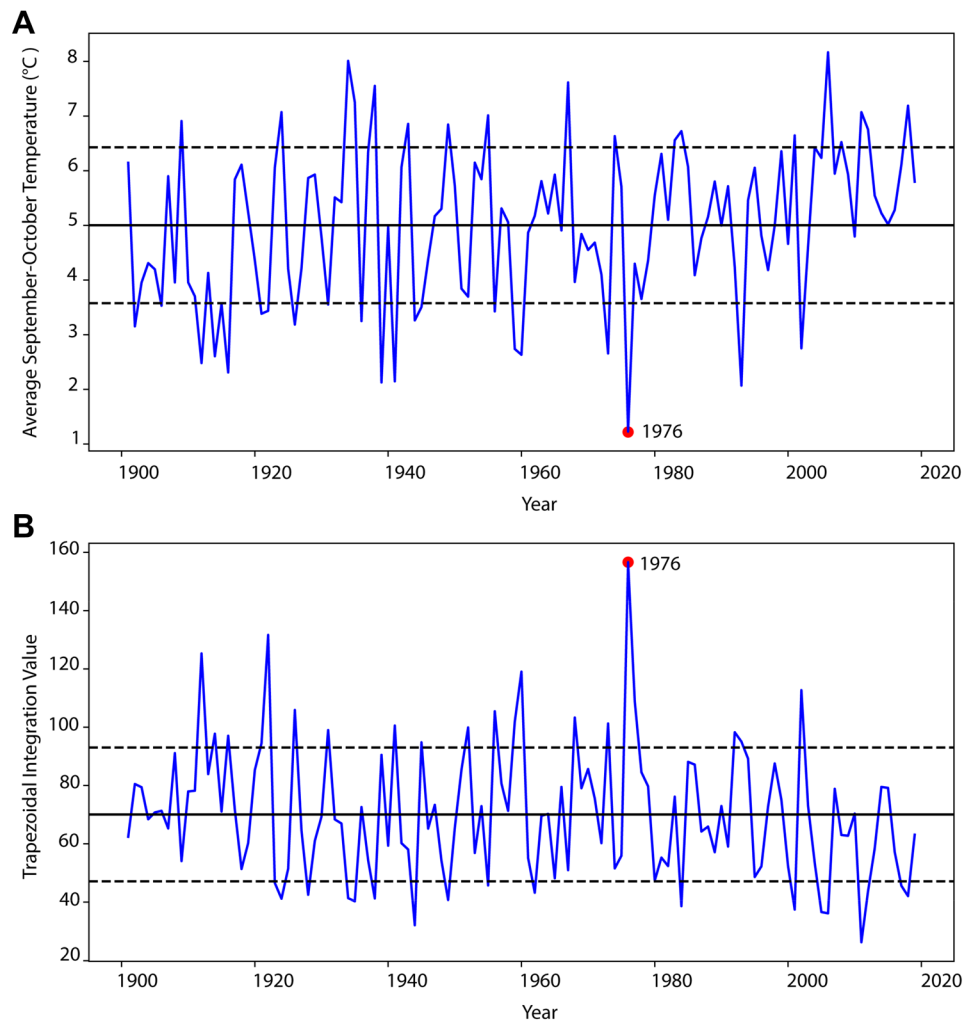
Positive phases of the NAO in the year 1976, outside of the interquartile range of the whole data set analysed, are found in March (z score = 0.95), May (z score = 0.93), June (z score = 1.55), and November (z score = 0.92), (Fig. 9). Negative phases of the NAO in 1976, outside of the interquartile range, occur in April (z score = -0.99), September (z score = -1.95) and December (z score = -2.11).

Significant positive correlations at $p < 0.01$ are found between the ARSTAN TRW chronology and monthly temperature in January, February, March, April and July. The pre-whitened ARSTAN TRW chronology showed significant correlations in the same months with the exception of July (Fig. 10). Both the original and pre-whitened ARSTAN BI chronologies show significant positive correlations ($p < 0.01$) with April and May temperatures. The pre-whitened BI ARSTAN chronology also presents significant correlations with June and September temperatures.

Discussion and conclusions

This study finds BRs occur in abundance, between and within trees, as a response triggered by a specific weather event at the end of the growing season, i.e., a cold spell

Fig. 7 **a** Mean minimum temperature ($^{\circ}\text{C}$) for September–October from the 1901–2019 period. **b** Absolute trapezoidal integration values below a temperature threshold of 5°C between September–October from 1901 to 2019. Both **a** and **b** were calculated from daily minimum temperatures ($^{\circ}\text{C}$) at Tõravere meteorological station. Solid black lines indicate the mean, dashed black lines represent one SD above and below the mean



which is extreme enough to inhibit the lignification of cell walls. At our sites in Estonia, from 1901 to 2019, only one year was prominent in this sense: 1976, in which BRs occurred in 78.6% of Scots pines, as well as at 100% of stem heights and directions in four of five whole-stem sample collections. Moreover, the trapezoidal analysis of end of growing season (September–October) temperatures revealed 1976 as an extreme cold anomaly, more than three SDs from the mean of the dataset. Both the average temperatures and trapezoidal integration results confirm that the September–October climate of 1976 contained the most significant exposure to below threshold temperatures of all the years recorded at Tõravere.

The summer of 1976 is renowned for a heatwave in Northwest Europe (Fig. 8a; Fischer et al. 2007), linked to a positive phase of the NAO (Fig. 9), and diffuent atmospheric blocking of westerly airflows associated with a North Atlantic jet stream anomaly (Woollings et al. 2018; Dorado-Liñán et al. 2022). Interestingly, following the summer

heatwave over Northwest Europe, Eastern Europe experienced an extreme cold anomaly in the September–October period (Fig. 8b), most likely linked to a strong negative phase of the NAO in September of the same year (Fig. 9). This extreme cold spell in the autumn of 1976 was captured by both the BRs and the meteorological record, yet not by TRW or BI (Fig. 6). Results from our temperature correlation analysis (Fig. 10) revealed a period of significant correlations between TRW and temperature in the winter months. This result may be explained by warmer winter temperatures enhancing metabolic processes, resulting in more productive subsequent growing seasons (Jacoby and D'arrigo 1989). TRW and BI correlations present before and early in the growing season may be linked to snow melt and increased water availability (Klippel et al. 2017). Despite some significant monthly temperature correlations, it appears that TRW and BI measurements do not respond to temperature during the growing season (Fig. 10). This is understandable given that the site is not near the thermal

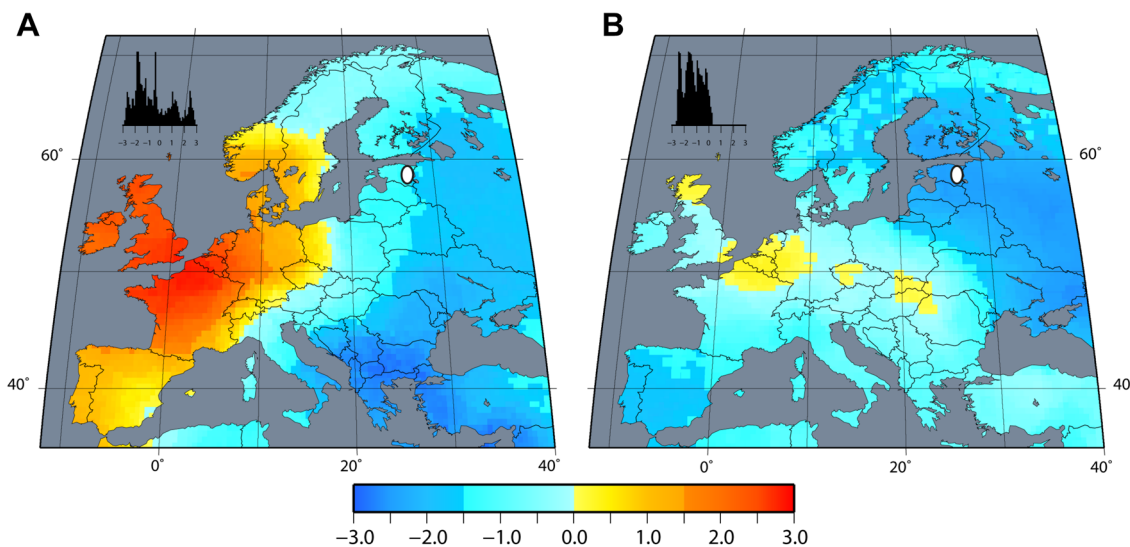
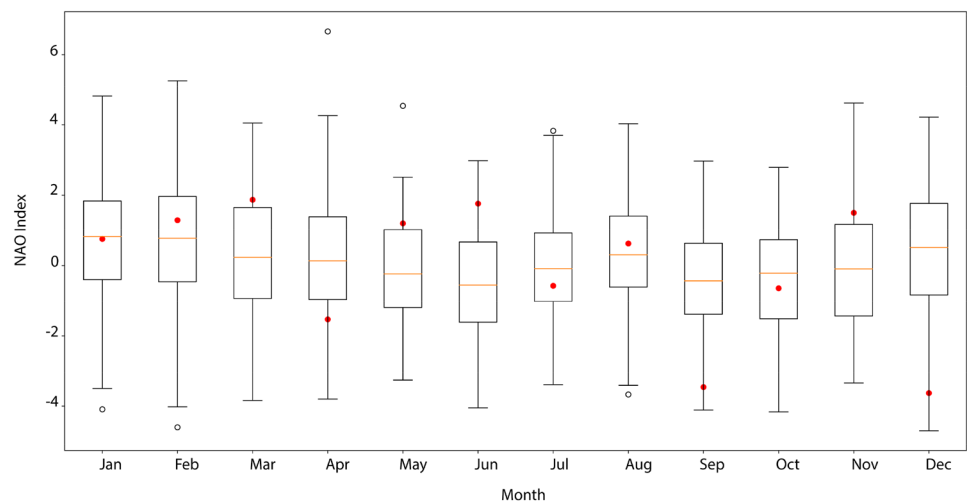


Fig. 8 Heat maps of Europe illustrating 1976 temperature anomalies (-3 to $+3$) calculated from Version 4 of the CRU TS dataset (Harris et al. 2020), with respect to the 1961–1990 period average temperatures in individual 0.5° latitude by 0.5° longitude grid cells. Histograms of temperature anomaly frequency shown in top left corner of

each map, study site in Estonia indicated by white ellipse. **a** Summer (June, July, August), **b** approximated end of growing season (September–October). Maps were completed using generic mapping tools (GMT) (Wessel and Smith 1991)

Fig. 9 Monthly North Atlantic Oscillation (NAO) index values calculated from normalised sea level pressure over Gibraltar and Southwest Iceland for 1901–2019, displayed as boxplots. The boxes represent the inter-quartile range of each month (25–75%), the orange line in the middle is the median value, the whiskers show the range of the data (after removing outliers), and outliers are shown using open circles. Values for 1976 are plotted for each month as solid red circles

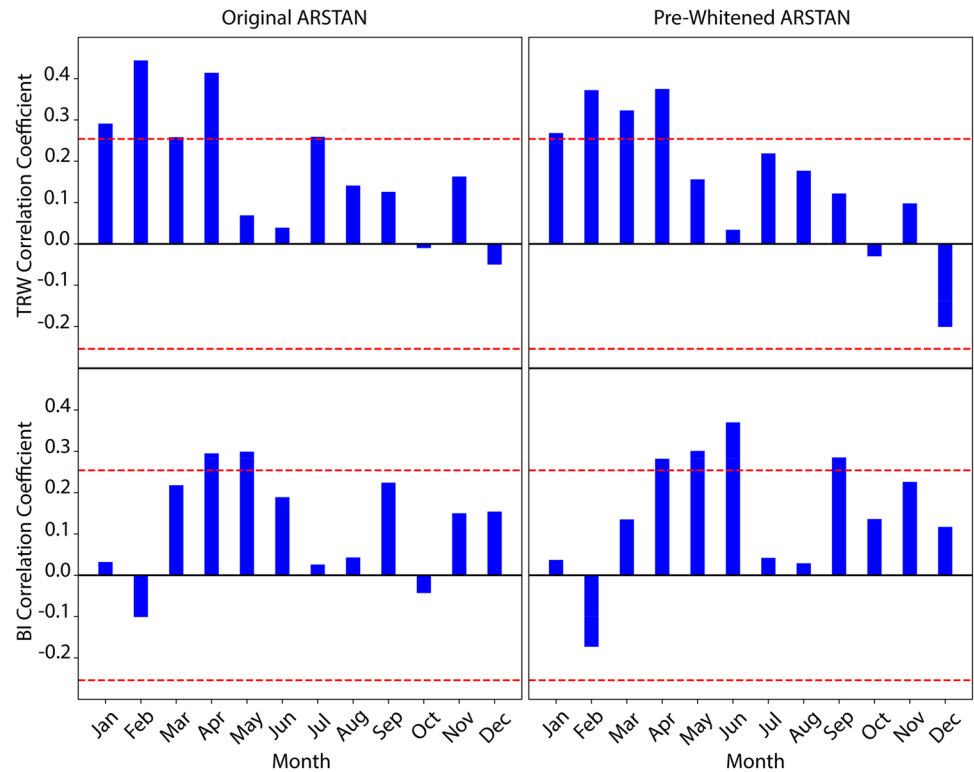


limit for Scots pine growth. Nevertheless, the wood anatomical response, indicated by BRs, evidently records the most extreme end of growing season cooling.

Our findings further demonstrate the link between late growing season temperatures and BR occurrence, as reported in previous work (Piermattei et al. 2015, 2020; Semeniuc et al. 2016; Montwé et al. 2018; Matisons et al. 2020; Tardif et al. 2020; Matulewski et al. 2022). Importantly, they show that BRs capture cooling episodes not evident in TRW or latewood density (e.g., BI) measurements (Piermattei et al. 2020). Our study provides further definition of what constitutes an extreme cold event based on

the abundance of BRs found both within and between trees. With the exception of 1976, all other BRs recorded display an irregular distribution between and within trees. It appears neither the formation nor within-tree distribution of these irregular BRs can be attributed to any specific temperature signal, at least, as our trapezoidal integration analysis suggests, not one as powerful as that which these Estonian Scots pines experienced in 1976. It is possible these BRs may be related to other biotic and abiotic stresses (Barros et al. 2015), the collection of multiple samples from larger numbers of trees will be required to identify those irregular BRs with limited paleoclimatic value.

Fig. 10 Pearson's correlation coefficients between monthly minimum temperatures from Tõravere meteorological station (1901–2019), and blue intensity (BI) and tree-ring width (TRW) ARSTAN chronologies (original and pre-whitened). The red dashed lines indicate significant correlations at $p < 0.01$



Since BRs can record cooling events not reflected in traditional dendrochronology or quantitative wood anatomy parameters, they may offer unique paleoclimatic insights into the short-term cooling following large volcanic eruptions (Piermattei et al. 2020; Büntgen et al. 2020; Tardif et al. 2020). BRs have also been considered as a potential tool for cross dating (Piermattei et al. 2015), though the results from this study regarding the distribution of BRs within the tree stem suggest such application should be approached with caution. Only the most extreme signals (e.g., 1976) look suitable for cross dating.

Limitations of our study include the quantification of BRs. Here, any ring containing some blue-stained cell walls was defined as a BR. Lacking differentiation of extent and frequency of blue cell walls (Fig. 3), or any qualitative or quantitative association between the degrees of BRs with climatic variables precludes the use of BRs beyond a binary indicator of late growing season cooling. Piermattei et al. (2020) did classify ‘partial BRs’ and more sophisticated image analysis may be able to quantify the varying intensities of BRs but even then, any relationship with degree of lignification has yet to be determined. Another limitation of this study is the definition of the end of a growing season. September–October is used here as previous studies have suggested thermal conditions during this period, in the Northern Hemisphere mid-latitudes, are relevant for the lignification of latewood tracheids (Gindl et al. 2000; Piermattei et al. 2015). In reality, though, both the onset

and cessation of the growing season can vary from year to year (Büntgen et al. 2022). However, defining the growing season with daily meteorological data presents new biases, thus, September–October is used as a conservative end of growing season window to enable comparisons throughout the time period studied.

As well as investigating the quantification of BRs, further research could consider the occurrence of BRs at sites with different meteorological conditions, for example, extreme sites with peripheral conditions for tree growth. Samples from these sites should be analysed alongside local high-resolution meteorological measurements to determine whether our findings are reproducible in other regions. The application of the trapezoidal rule (Fig. 4) may enable future studies to further constrain the intensity, duration and timing of cool spells necessary to initiate consistent BR formation. Furthermore, the occurrence of BRs in more tree species must be evaluated, as well as the influence of different environmental conditions such as soil type. Whilst this study included samples from peat and mineral soil sites, the number of peat site samples was insufficient for any significant comparisons.

There is no question that the September–October period over Estonia in 1976 was extremely cold, and this had a demonstrable effect on late growing season cell wall lignification. What remains unclear is the role of species and site-specific variables in determining the temperature thresholds that trigger BR formation. Without this knowledge it will

be difficult to use BRs as anything more than an elusive categorical climate proxy.

Acknowledgements This study was supported by the Estonian Ministry of Education and Research (project SF0170014s08), Estonian Science Foundation (Grant 8890), Järvseja Training and Experimental Forest Centre, Estonian Environmental Investment Centre, Estonian University of Life Sciences ASTRA project “Value-chain based bio-economy” (supported by the European Union, European Regional Development Fund). CG received funding from Natural Environment Research Council—United Kingdom Research and Innovation. UB received funding from the SustES project—Adaptation strategies for sustainable ecosystem services and food security under adverse environmental conditions (CZ.02.1.01/0.0/0.0/16_019/0000797), and the ERC Advanced project Monostar (AdG 882727). S.M received funding from the Estonian University of Life Sciences project P200189MIMP.

Author contribution statement A.P(otapov), M.H, R.K, S.M and A.K conducted fieldwork to collect samples, A.P(otapov) and A.C performed the wood anatomical analysis, and C.G and A.P(iermattei) produced blue intensity measurements. C.G, A.P(otapov), A.C, A.P(iermattei), U.B and P.J.K designed the study. C.G produced the first draft of this manuscript with input from P.J.K and U.B, all other authors contributed to improving the article.

Funding Funding was provided by Estonian Ministry of Education and Research (SF0170014s08), Estonian Science Foundation (grant 8890), European Union, European Regional Development Fund, Natural Environment Research Council, SustES project (CZ.02.1.01/0.0/0.0/16_019/0000797), ERC Advanced project Monostar (AdG 882727).

Data availability statement The datasets produced in this study are available from the corresponding author, [C.G], upon reasonable request.

Declarations

Competing interests The authors have no relevant financial or non-financial conflicts of interests.

Open Access This article is licensed under a Creative Commons Attribution 4.0 International License, which permits use, sharing, adaptation, distribution and reproduction in any medium or format, as long as you give appropriate credit to the original author(s) and the source, provide a link to the Creative Commons licence, and indicate if changes were made. The images or other third party material in this article are included in the article's Creative Commons licence, unless indicated otherwise in a credit line to the material. If material is not included in the article's Creative Commons licence and your intended use is not permitted by statutory regulation or exceeds the permitted use, you will need to obtain permission directly from the copyright holder. To view a copy of this licence, visit <http://creativecommons.org/licenses/by/4.0/>.

References

- Barros J, Serk H, Granlund I, Pesquet E (2015) The cell biology of lignification in higher plants. *Ann Bot* 115(7):1053–1074
- Björklund J, Arx G, Nievergelt D, Wilson R, Van den Bulcke J, Günther B, Loader N, Rydval M, Fonti P, Scharnweber T, Andreu-Hayles L, Büntgen U, D'Arrigo R, Davi N, De Mil T, Esper J, Gärtner H, Geary J, Gunnarson B, Hartl C, Hevia A, Song H, Janecka K, Kaczka R, Kirdyanov A, Kochbeck M, Liu Y, Meko M, Mundo I, Nicolussi K, Oelkers R, Pichler T, Sánchez-Salguero R, Schneider L, Schweingruber F, Timonen M, Trouet V, Van Acker J, Verstege A, Villalba R, Wilmking M, Frank D (2019) Scientific merits and analytical challenges of tree-ring densitometry. *Rev Geophys* 57(4):1224–1264
- Björklund J, Fonti M, Fonti P, Van den Bulcke J, von Arx G (2021) Cell wall dimensions reign supreme: cell wall composition is irrelevant for the temperature signal of latewood density/blue intensity in Scots pine. *Dendrochronologia* 65:125785
- Büntgen U, Arseneault D, Boucher É, Churakova O, Gennaretti F, Crivellaro A, Hughes M, Kirdyanov A, Klippel L, Krusic PJ, Linderholm H, Jungqvist F, Ludescher J, McCormick M, Myglan V, Nicolussi K, Piermattei A, Oppenheimer C, Reinig F, Sigl M, Vaganov E, Esper J (2020) Prominent role of volcanism in common era climate variability and human history. *Dendrochronologia* 64:125757
- Büntgen U, Piermattei A, Krusic PJ, Esper J, Sparks T, Crivellaro A (2022) Plants in the UK flower a month earlier under recent warming. *Proc R Soc B* 289:20212456
- Cabon A, Peters R, Fonti P, Martínez-Vilalta J, De Cáceres M (2020) Temperature and water potential co-limit stem cambial activity along a steep elevational gradient. *New Phytol* 226(5):1325–1340
- Cook ER, Krusic PJ, Peters K, Holmes RL (2017) Program ARSTAN (ver. 49v1), Autoregressive tree-ring standardization program. Tree-Ring Laboratory of Lamont-Doherty Earth Observatory, Palisades
- Cook ER (1985) A time series analysis approach to tree ring standardization. Ph.D. thesis, The University of Arizona
- Crivellaro A, Büntgen U (2020) New evidence of thermally constrained plant cell wall lignification. *Trends Plant Sci* 25(4):322–324
- Crivellaro A, Reverenna M, Ruffinatto F, Urbinati C, Piermattei A (2018) The anatomy of “blue ring” in the wood of *Pinus nigra*. *Les/wood* 67(2):21–28
- Crivellaro A, Piermattei A, Dolezal J, Dupree P, Büntgen U (2022) Biogeographic implication of temperature-induced plant cell wall lignification. *Commun Biol* 5(1):1–10
- Dorado-Liñán I, Ayarzagüena B, Babst F, Xu G, Gil L, Battipaglia G, Buras A, Čada V, Camarero J, Cavin L, Claessens H, Drobyshev I, Garamszegi B, Grabner M, Hacket-Pain A, Hartl C, Hevia A, Janda P, Jump A, Kazimirovic M, Keren S, Kreyling J, Land A, Latte N, Levanič T, van der Maaten E, van der Maaten-Theunissen M, Martínez-Sancho E, Menzel A, Mikoláš M, Motta R, Muffler L, Nola P, Panayotov M, Petritan A, Petritan I, Popa I, Prislan P, Roibu C, Rydval M, Sánchez-Salguero R, Scharnweber T, Stajić B, Svoboda M, Tegel W, Teodosiu M, Toromani E, Trotsiuk V, Turcu D, Weigel R, Wilmking M, Zang C, Zlatanov T, Trouet V (2022) Jet stream position explains regional anomalies in European beech forest productivity and tree growth. *Nat Commun* 13(1):1–10
- Fischer E, Seneviratne S, Lüthi D, Schär C (2007) Contribution of land-atmosphere coupling to recent European summer heat waves. *Geophys Res Lett* 34(6):1–6
- Fritts HC (1976) Tree rings and climate. Academic Press, London
- Gärtner H, Nievergelt D (2010) The core-microtome: a new tool for surface preparation on cores and time series analysis of varying cell parameters. *Dendrochronologia* 28(2):85–92
- Gärtner H, Cherubini P, Fonti P, von Arx G, Schneider L, Nievergelt D, Verstege A, Bast A, Schweingruber FH, Büntgen U (2015) Technical challenges in tree-ring research including wood anatomy and dendroecology. *J vis Exp* 97:e52337
- Gerlach D (1984) Botanische Mikrotechnik, 3rd edn. Thieme, Stuttgart
- Gindl W, Grabner M, Wimmer R (2000) The influence of temperature on latewood lignin content in treeline Norway spruce

- compared with maximum density and ring width. *Trees Struct Funct* 14(7):409–414
- Harris I, Osborn T, Jones P, Lister D (2020) Version 4 of the CRU TS monthly high-resolution gridded multivariate climate dataset. *Sci Data* 7(1):1–18
- Holmes RL (1983) Computer-assisted quality control and tree ring dating and measurement. *Tree-Ring Bull* 43:69–77
- Jacoby G, D'Arrigo R (1989) Reconstructed Northern Hemisphere annual temperature since 1671 based on high-latitude tree-ring data from North America. *Clim Change* 14(1):39–59
- Jones P, Jonsson T, Wheeler D (1997) Extension to the North Atlantic oscillation using early instrumental pressure observations from Gibraltar and south-west Iceland. *Int J Climatol* 17(13):1433–1450
- Klippel L, Krusic P, Brandes R, Hartl-Meier C, Trouet V, Meko M, Esper J (2017) High-elevation inter-site differences in Mount Smolikas tree-ring width data. *Dendrochronologia* 44:164–173
- Körner C (2008) Winter crop growth at low temperature may hold the answer for alpine treeline formation. *Plant Ecol Divers* 1(1):3–11
- Körner C (2021) The cold range limit of trees. *Trends Ecol Evol* 36(11):979–989
- Krusic PJ, Kenney M, Hornbeck J (1987) Preparing increment cores for ring-width measurements. *North J Appl* 4(2):104–105
- Matisons R, Gärtner H, Elferts D, Kärkliņa A, Adamovičs A, Jansons Ā (2020) Occurrence of ‘blue’ and ‘frost’ rings reveal frost sensitivity of eastern Baltic provenances of Scots pine. *For Ecol Manag* 457:117729
- Matulewski P, Buchwal A, Gärtner H, Jagodziński A, Čufar K (2022) Altered growth with blue rings: comparison of radial growth and wood anatomy between trampled and non-trampled Scots pine roots. *Dendrochronologia* 72:125922
- Maxwell R, Larsson L (2021) Measuring tree-ring widths using the CooRecorder software application. *Dendrochronologia* 67:125841
- McCarroll D, Pettigrew E, Luckman A, Guibal F, Edouard J (2002) Blue reflectance provides a surrogate for latewood density of high-latitude pine tree rings. *Arct Antarct Alp Res* 34(4):450–453
- Metslaid S, Sims A, Kangur A, Hordo M, Jõgiste K, Kiviste A, Hari P (2011) Growth patterns from different forest generations of Scots pine in Estonia. *J for Res* 16(3):237–243
- Montwé D, Isaac-Renton M, Hamann A, Spiecker H (2018) Cold adaptation recorded in tree rings highlights risks associated with climate change and assisted migration. *Nat Commun* 9(1):1–7
- Parker ML, Jozsa LA (1973) X-ray scanning machine for tree-ring width and density analysis. *Wood Fiber Sci* 5(3):192–197
- Piermattei A, Crivellaro A, Carrer M, Urbinati C (2015) The “blue ring”: anatomy and formation hypothesis of a new tree-ring anomaly in conifers. *Trees Struct Funct* 29(2):613–620
- Piermattei A, Crivellaro A, Krusic PJ, Esper J, Vitek P, Oppenheimer C, Felhofer M, Gierlinger N, Reinig F, Urban O, Verstege A, Lobo H, Büntgen U (2020) A millennium-long ‘Blue Ring’ chronology from the Spanish Pyrenees reveals severe ephemeral summer cooling after volcanic eruptions. *Environ Res Lett* 15(12):124016
- Potapov A, Toomik S, Yermokhin M, Edvardsson J, Lilleleht A, Kiviste A, Kaart T, Metslaid S, Järvel A, Hordo M (2019) Synchronous growth releases in peatland pine chronologies as an indicator for regional climate dynamics—a multi-site study including Estonia, Belarus and Sweden. *Forests* 10(12):1097
- Rossi S, Deslauriers A, Anfodillo T, Morin H, Saracino A, Motta R, Borghetti M (2006) Conifers in cold environments synchronize maximum growth rate of tree-ring formation with day length. *New Phytol* 170:301–310
- Rydval M, Larsson L, McGlynn L, Gunnarson B, Loader N, Young G, Wilson R (2014) Blue intensity for dendroclimatology: should we have the blues? Experiments from Scotland. *Dendrochronologia* 32(3):191–204
- Schenker G, Lenz A, Körner C, Hoch G (2014) Physiological minimum temperatures for root growth in seven common European broad-leaved tree species. *Tree Physiol* 34(3):302–313
- Schweingruber FH (2007) Wood structure and environment. Springer, Berlin, p 271
- Schweingruber FH, Fritts HC, Bräker OU, Drew LG, Schär E (1978) The X-ray technique applied to dendroclimatology. *Tree-Ring Bull* 38:61–91
- Semeniuc A, Sidor C, Popa I (2016) Scots pine tree ring structure modifications and relation with climate. *Eurasian J for Sci* 4(2):1–7
- Tardif J, Salzer M, Conciatori F, Bunn A, Hughes M (2020) Formation, structure and climatic significance of blue rings and frost rings in high elevation bristlecone pine (*Pinus longaeva* D.K. Bailey). *Quat Sci Rev* 244:106516
- Tumajer J, Kašpar J, Kuželová H, Shishov V, Tychkov I, Popkova M, Vaganov E, Treml V (2021) Forward modeling reveals multidecadal trends in cambial kinetics and phenology at treeline. *Front Plant Sci* 12:1–14
- Wessel P, Smith W (1991) Free software helps map and display data. *Eos Trans Am Geophys Union* 72(41):441–441
- Woollings T, Barriopedro D, Methven J, Son S, Martius O, Harvey B, Sillmann J, Lupo A, Seneviratne S (2018) Blocking and its response to climate change. *Curr Clim Change Rep* 4(3):287–300
- Yeh K, Kwan K (1978) A comparison of numerical integrating algorithms by trapezoidal, Lagrange, and spline approximation. *J Pharmacokinet Biopharm* 6(1):79–98

Publisher's Note Springer Nature remains neutral with regard to jurisdictional claims in published maps and institutional affiliations.